

# Diffusion Kurtosis Imaging Shows Similar Cerebral Axonal Damage in Patients with HIV Infection and Multiple Sclerosis

Korhan Buyukturkoglu, Lazar Fleyser, Desiree Byrd, Susan Morgello, Matilde Inglese

From the Department of Neurology (KB, SM, MI), Icahn School of Medicine at Mount Sinai, New York, NY; Radiology (LF, MI), Icahn School of Medicine at Mount Sinai, New York, NY; Pathology (SM), Icahn School of Medicine at Mount Sinai, New York, NY; Psychiatry (DB), Icahn School of Medicine at Mount Sinai, New York, NY; Neuroscience (SM, MI), Icahn School of Medicine at Mount Sinai, New York, NY; and Department of Neuroscience, Rehabilitation, Ophthalmology, Genetics, Maternal and Child Health (DINOGLM), University of Genoa, Genoa, Italy (MI).

## ABSTRACT

**BACKGROUND AND PURPOSE:** In this pilot study, we sought to investigate the pathological changes in the white matter (WM) of medically complex, combination antiretroviral therapy (cART)-treated patients with human immunodeficiency virus (HIV), comparing them to patients with long-standing, secondary progressive multiple sclerosis (SPMS).

**METHODS:** Using diffusion kurtosis imaging (DKI)-derived WM tract integrity (WMTI) metrics, 15 HIV and 15 age- and sex-matched SPMS patients with similar disease duration underwent magnetic resonance imaging analysis. Maps of WMTI metrics were created. Tract-based spatial statistics analysis of the whole brain and regions of interest analysis of the corpus callosum (CC) and the anterior thalamic radiations (ATRs) were performed and the derived WMTI metrics were compared between the groups of patients.

**RESULTS:** Axonal water fraction, an index of chronic axonal loss, showed similarities between HIV and the chronic MS patients in all regions; in contrast, tortuosity, a measure more sensitive to myelin loss, was regionally variable. In addition, in HIV patients, WMTI metrics of the CC and left ATR were associated with cognitive test scores, suggesting clinical relevance for these measures of WM damage.

**CONCLUSIONS:** We conclude that DKI-derived WMTI metrics may be a valuable tool in assessing the WM changes of medically complex HIV-infected individuals. While not powered to examine potential etiologies of WM changes in this pilot sample, regional variations in WMTI metrics were seen. When contrasted with changes consequent to chronic MS of similar duration, HIV and its comorbidities appear to result in similar degrees of axonal damage, but regionally variable amounts of myelin loss and extraxonal abnormality.

**Keywords:** HIV, multiple sclerosis, diffusion kurtosis imaging.

**Acceptance:** Received September 16, 2017. Accepted for publication December 21, 2017.

**Correspondence:** Address correspondence to Matilde Inglese, Radiology and Neuroscience, Icahn School of Medicine at Mount Sinai, Annenberg 14, Box 1137, One Gustave L. Levy Place, New York, NY 10029. E-mail: matilde.inglese@mssm.edu.

**Acknowledgments and disclosures:** This work was supported by grant U24MH100931 (The Manhattan HIV Brain Bank) from the National Institutes of Health, and a pilot research grant from the Icahn School of Medicine Brain Imaging Center to SM and by a grant from the National Multiple Sclerosis Society (NMSS RG 5120A3/1) to MI. The authors have no financial conflicts of interest to disclose.

J Neuroimaging 2018;00:1-8.  
DOI: 10.1111/jon.12497

## Introduction

Human immunodeficiency virus (HIV) infects cells of the immune system and crosses the blood-brain barrier soon after seroconversion, inducing the activation of central nervous system (CNS) cells of the monocyte-macrophage lineage.<sup>1</sup> Previous studies have shown that brain infiltration by immune cells may cause axonal disruption, synaptic injury, decrease of the myelin sheath thickness and/or frank myelin loss, astrogliosis, and, in rare cases, extensive destruction of the white matter (WM) tracts.<sup>2-5</sup> HIV-associated WM abnormalities are diffuse, but often involve frontal WM and cortical-subcortical pathways, and may disrupt the functional connectivity between the basal ganglia, thalamus, and neocortex.<sup>2</sup> Approximately 50% of patients with HIV are diagnosed with neurocognitive disorders, which may, in part, reflect WM abnormality.<sup>5-8</sup> HIV-associated neurocognitive disorder (HAND) is characterized by deficits of attention, memory, executive function, information processing speed, and decision-making,<sup>9</sup> whose severity ranges

from asymptomatic and mild impairment to HIV-associated dementia.

Consequent to the availability of combination antiretroviral therapy (cART), our understanding of both WM abnormalities and cognitive/behavioral deficits in individuals with HIV has become more complicated. As individuals age on virally suppressive therapies, they develop comorbid medical disorders that in and of themselves may result in WM damage and cognitive change, such as hypertension (HTN), diabetes mellitus (DM), and chronic liver disease. Furthermore, there have been suggestions that some ART regimens may be associated with WM damage.<sup>10</sup> Thus, techniques allowing a deeper understanding of the pathogenesis of WM changes in HIV are needed.

Diffusion tensor imaging (DTI) is a noninvasive imaging method that quantifies the magnitude and directionality of tissue water mobility and provides a unique tool to study WM abnormalities in vivo.<sup>11</sup> Recent studies have found DTI to be superior to conventional magnetic resonance imaging (MRI)

in detecting WM abnormalities and predicting the severity of HAND.<sup>9</sup> Diffusion kurtosis imaging (DKI) is an extension of DTI that enables the quantification of non-Gaussian diffusion through the estimation of the diffusional kurtosis.<sup>12</sup> DKI allows for the quantification of WM tract integrity (WMTI) metrics such as intra- and extra-axonal diffusivities, axonal water fraction, and tortuosity,<sup>12</sup> which have been shown to be more specific than standard DTI to pathological processes in both experimental models and neurological diseases.<sup>13–18</sup> In a recent study, we have applied the WMTI technique to patients with multiple sclerosis (MS) who are characterized by extensive and pathologically heterogeneous abnormalities of the WM. We have found that radial extra-axonal diffusivity was significantly increased, while axonal water fraction, intra-axonal diffusivity, and tortuosity were decreased in MS patients compared with controls.<sup>17</sup> With the exception of the axial extra-axonal diffusivity, all metrics were correlated with the symbol digit modality test score (*P* values ranging from .001 to <.05), suggesting that not only are WMTI metrics sensitive to changes in the WM of MS patients but also clinically relevant.

Accordingly, we sought to characterize the nature and extent of pathological changes in the WM of complex patients with HIV using novel DKI-derived WMTI metrics and to compare them with those of MS patients with chronic course and long disease duration. While HIV is not a primarily demyelinating disorder, it does share with MS features of myelin and axonal damage, as demonstrated in prior neuroimaging studies.<sup>19</sup> Moreover, in order to investigate the clinical relevance of WM abnormalities in HIV patients, we tested the association between WMTI metrics measured in the corpus callosum (CC) and anterior thalamic radiations (ATRs) and patients' cognitive performance. We focused our analysis on the CC because it is a prominent, homogeneous dense WM tract that has been extensively examined in HIV and MS patients<sup>18,20–22</sup> and on the ATRs because it is one of the sites of predilection for radiologically defined HIV WM tract pathology.<sup>5,23</sup>

## Methods

Eighteen HIV-positive patients were prospectively enrolled in this study. MRI Data from 3 HIV patients were excluded from the analysis due to significant motion artifacts. Thus, data from 15 HIV patients (mean age:  $55.1 \pm 6.4$ , mean disease duration:  $21.8 \text{ years} \pm 5.5$ ) were compared with those of 15 age and gender matched patients with secondary-progressive MS (SPMS) (mean age:  $57.1 \pm 7.2$ , mean disease duration:  $17.6 \pm 10.6$ ). Demographic and clinical characteristics of the study groups are presented in Table 1.

### *Inclusion and Exclusion Criteria for HIV Patients*

The HIV positive individuals were recruited to an Icahn School of Medicine Brain Imaging Center-sponsored pilot study from the ongoing cohort studies of one of the coauthors (SM), the Manhattan HIV Brain Bank (MHBB; U24MH100931). The intent of the pilot study was to perform a neuroimaging analysis of a heterogeneous sample of chronically HIV-infected individuals who had undergone extensive neurocognitive, neurologic, and medical assessment, for the purposes of determining whether chronic administration of maintenance opioids had impacts on neurometabolites or brain structure. Accordingly, recruitment criteria were broad: HIV-positive; participating

in the ongoing cohort study; either on or off chronic opioid therapy as demonstrated by urine toxicology testing; ability to undergo neuroimaging within a month of the primary study visit in which cognitive characterization was performed; and on stable cART therapy for a minimum of 3 months. Patients were medically and cognitively heterogeneous. Exclusion criteria were contraindications for MRI and pregnancy. All subjects provided written informed consent, and the research was overseen by the Mount Sinai Program for the Protection of Human Subject Institutional Review Board.

### *Inclusion and Exclusion Criteria for SPMS Patients*

MRI data were obtained from MS patients recruited from an ongoing longitudinal study funded by the National MS Society to identify MRI markers of disease progression in patients with progressive MS. Only MRI data from MS patients with secondary-progressive course<sup>24</sup> and matched for age and sex with the HIV patients were used for MRI comparisons.

Exclusion criteria for all subjects were: (i) contraindications to MRI (metal in the body, claustrophobia), (ii) pregnancy, and (iii) large body habitus.

### *Clinical Data Collection in HIV Patients*

Patients were assessed by clinical interview, review of the medical record, and laboratory testing as part of the MHBB protocol. Routine MHBB laboratories include: hepatitis B and C serologies, CD4<sup>+</sup> T lymphocyte counts, HIV plasma load, and urine toxicology. Urine toxicology screened for amphetamines, barbiturates, benzodiazepines, cannabinoids, cocaine, opiates, phencyclidine, methadone, and propoxyphene. The presence or absence of HTN, diabetes, obesity, hyperlipidemia, and historical herpes infections (herpes simplex virus, varicella-zoster virus, and cytomegalovirus) was ascertained by interview and review of medications and the medical record.

### *Neuropsychological and Psychiatric Assessment in HIV Patients*

The neuropsychological tests used for this study were selected from a larger battery of tests as previously described.<sup>6,25</sup> The Trail Making Test, Part A (TMT-A) was selected as a measure of information processing speed; the Brief Visuospatial Memory Test-Revised (BVMT-R) as a measure of visual-spatial memory and the Trail Making Test, Part B (TMT-B) as a measure of executive functions. In order to minimize the processing speed component, TMT-B was regressed on TMT-A and the residual values were used for analyses. Raw scores from all tests were converted to demographically adjusted T-scores taking into account the effects of age, sex, and education.<sup>26</sup> We conducted this preliminary analysis to determine whether, like conventional DTI, there might be a suggestion of clinical relevance to our parameters, and to determine which elements of our methodology might show indication of potential correlation. Our choice of individual cognitive tests was not meant to be comprehensive, but to select measures in cognitive domains that continue to be impacted in cART-era HIV disease; learning and executive functioning in particular appear to have increased in cART era populations relative to pre-cART.<sup>8</sup>

### *MRI Acquisition*

All subjects underwent MRI on a 3T Siemens Skyra scanner (Siemens Medical Solutions, Erlangen, Germany) with a

Table 1. Demographic and Clinical Characteristics of the Study Groups

	HIV	SPMS	P Value
Age	Mean (SD) 55.1 ± 6.4 Median 56 (Range: 41–65)	Mean (SD) 57.1 ± 7.2 Median 57 (Range: 46–73)	.51
Sex	12 F, 3 M	10 F, 5 M	.42
Disease duration	Mean (SD) 21.8 ± 5.5 Median 23 (Range: 13–30)	Mean (SD) 17.6 ± 10.6 Median 13 (Range: 8–49)	.17
<b>Clinical Features of Disease</b>			
EDSS	Not available	Median 6.0 (Range: 3.0–8.5)	-
Comorbidities	Hepatitis C virus infection (5 patients) Hypertension (6 patients) Diabetes (4 patients)	None	-
CD4 count	Median [IQR] 660 [399, 922] (Range: 33–1,023)	Not available	-
Nadir CD4 count	Median [IQR] 22 [5, 225] (Range: 1–850)	Not available	-
Plasma HIV load	Median [IQR] 21 [0, 95] copies/mL	Not available	-
Chronic opioid use	8 patients (5 on methadone treatment)	None	-

HIV = human immunodeficiency virus; SPMS = secondary progressive multiple sclerosis; EDSS = expanded disability status scale; SD = standard deviation; IQR = interquartile range; M = male; F = female.

Table 2. MRI Acquisition Parameters

MRI Acquisition Parameters	DKI	3D-T2	3D-T1 MPRAGE
Plane	Axial	Sagittal	Sagittal
TE (milliseconds)	100	566	1.99
TR (milliseconds)	4,700	3,200	2,400
Flip angle	80°	N/A	8°
Number of signal averages	6	1	1
Field of view (mm × mm)	224 × 189	256 × 256	224 × 224
Voxel size (mm × mm × mm)	1.8 × 1.8 × 1.8	1 × 1 × 1	1 × 1 × 1
Number of slices	78	176	176
Slice thickness (mm)	1.8	1	1
<i>b</i> -Value (seconds/mm <sup>2</sup> )	0/1,000/2,000	N/A	N/A
Number of gradient directions	30	N/A	N/A
Acquisition time	15 minutes	4.46 minutes	5.35 minutes

DKI = diffusion kurtosis imaging; 3D T2 = 3-dimensional T2-weighted imaging; 3D T1MPRAGE = 3-dimensional T1-weighted magnetization-prepared rapid gradient-echo imaging; TE = echo time; TR = repetition time; N/A = not applicable.

16-channel head coil for reception. The MRI protocol included: (a) 3D T1-weighted MPRAGE (TR/TE/TI: 2,400/1.99/1,000 milliseconds; voxel size: 1 mm<sup>3</sup>; 176 slices); (b) 3D T2-weighted space (TR/TE: 3,200/566 milliseconds; FoV: 256 × 256; matrix: 256 × 256; slice thickness: 1 mm; 176 slices); (c) multiband accelerated EPI sequence for DKI (TR/TE = 4,700/100 milliseconds; FoV: 224 × 189 mm; FA: 80°; matrix: 128 × 108; voxel size: 1.75 × 1.75; slice thickness: 1.8 mm; multiband acceleration factor 3), 30 diffusion encoding directions with *b* values: 0, 1,000, 2,000 seconds/mm<sup>2</sup>. To correct the field inhomogeneity and to improve the signal to noise ratio (SNR), data were acquired twice with alternating phase-encoding directions (left/right, right/left). In addition, *b* = 0 images were averaged six times for each left/right and right/left phase-encoding directions. DKI approach was not used to compute conventional DTI metrics. These metrics were estimated from *b* = 0 and *b* = 1,000 data only. Details of the acquisition parameters are presented in Table 2.

## MRI Analysis

### Lesion Volume Measurements in HIV and MS Patients

T2 hyperintense lesion volume (T2-LV) measurements were performed using a semiautomatic segmentation technique based on local thresholding (Jim version 6, Xinapse Systems, Essex, UK, <http://www.xinapse.com>).<sup>27</sup>

### Diffusion Imaging and White Matter Integrity Metrics

Diffusion MRI data were transferred to an offline workstation and processed using in-house developed software<sup>17</sup> and the Oxford Centre for Functional MRI of the Brain (FMRIB)'s Diffusion Toolbox within FSL 5.0.7. Motion, eddy current, and field inhomogeneity corrections were performed in FSL.<sup>28–30</sup> *b* = 0 images were used to extract the brain by using BET function from FSL.<sup>31</sup> Based on the previously introduced model,<sup>12</sup> using diffusional kurtosis estimator (DKE) software<sup>32</sup> (version

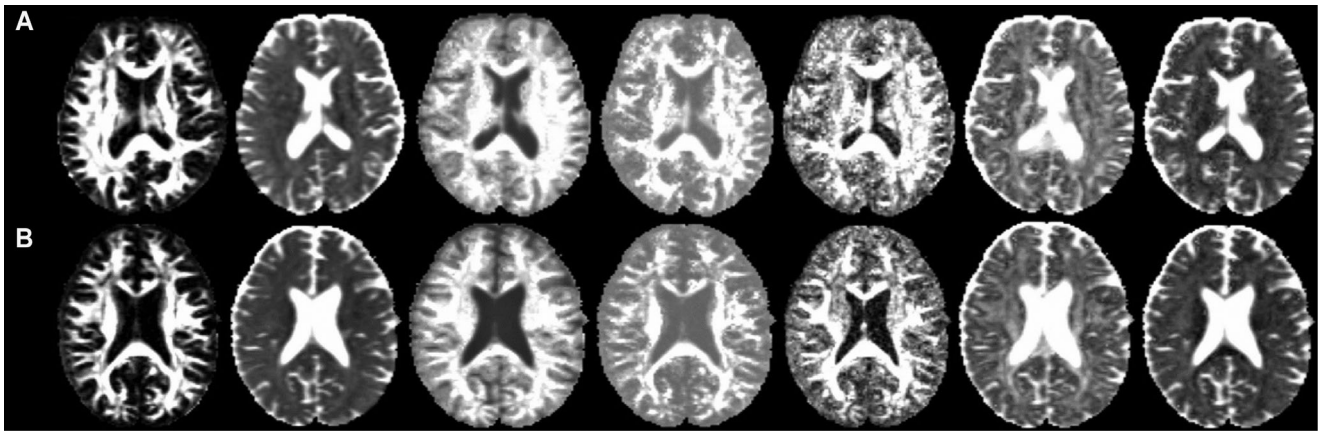


**Fig 1.** From left to right, fractional anisotropy, mean diffusivity, axonal water fraction, tortuosity, intra-axonal diffusivity, axial extra-axonal diffusivity, and radial extra-axonal diffusivity maps of (A) an HIV patient and (B) a secondary progressive multiple sclerosis patient.

2.5.0) conventional DTI metrics (FA, MD), and the following DKI metrics were derived:

- Axonal water fraction (AWF, which represents the ratio of water within the intra-axonal space over the total amount of water (i.e., water in the intra- and extra-axonal space). This metric is thought to be a potential marker of chronic axonal loss.
- Tortuosity of the extra-axonal space, which is defined as the ratio of intrinsic diffusivity in the extra-axonal space over diffusivity in the extra-axonal space perpendicular to axonal tracts. Tortuosity is thought to be a marker of demyelination.
- The intra-axonal diffusivity ( $D_{\text{axon}}$ ), which corresponds to the diffusivity of water inside of axons. This metric is considered as a potential marker of acute intra-axonal injury.
- The axial and radial extra-axonal diffusivities ( $D_{\text{e,axial}}$  and  $D_{\text{e,radial}}$ , respectively), which quantify diffusivity in the extracellular space parallel (i.e., axial) to and perpendicular (i.e., radial) to axonal tracts. These metrics are specific for extra-axonal processes and are considered as potential markers of extracellular inflammation, gliosis, and demyelination.<sup>12,17</sup>

AWF and tortuosity values were calculated with the additional tools provided by the authors of the software. Figure 1 shows representative maps of above-mentioned metrics for an HIV and SPMS patient.

#### *Tract-Based Spatial Statistical Analysis (TBSS)*

Voxelwise statistical analysis of the FA data was carried out using TBSS (Tract-Based Spatial Statistics),<sup>33</sup> part of FSL (FMRI Software Library).<sup>34</sup> All subjects' FA maps were registered to FMRIB58 FA template with the nonlinear registration tool FNIRT<sup>35</sup> and resampled to  $1 \times 1 \times 1 \text{ mm}^3$  Montreal Neurological Institute space. All other parametric maps underwent the same transformations for subsequent processing. Next, a mean FA image was created and thinned to create a mean FA skeleton representing the centers of all tracts common to the group. The FA skeleton was thresholded to  $\text{FA} \geq .2$  to restrict further analysis to WM regions consisting of single-fiber bundles. All parametric maps of each subject were then projected onto this FA skeleton for further skeletonized voxelwise statistical analysis. TBSS analysis was performed across all voxels on the skeleton by using a permutation-based inference tool for nonparametric statistical thresholding (randomize; FSL). The comparison between HIV and SPMS patients in terms of all parameters within the skeleton was tested by using *t* tests, with subject age and sex as a covariate. The number of permutations

was set to 5,000. The resulting statistical maps were thresholded (two-sided  $P < .05$ ), with correction for multiple comparisons included by using the threshold-free cluster enhancement option.<sup>36</sup> Additionally, lesion masks were created for each patient on axial FLAIR images, transformed in standard space and averaged to create a mean lesion mask across all patients. This was then thresholded to include only voxels in which at least 10% of patients had a lesion.

#### *Region of Interest Analysis*

Regions of interest (ROI) analysis was performed to investigate group differences between HIV and SPMS patients and correlations between DKI-derived metrics and measures of cognitive impairment in HIV patients. ROI analysis was restricted to the CC and to the ATRs (Fig 2). The CC is a prominent, homogeneous dense WM tract and has been extensively examined in HIV and MS patients in previous studies.<sup>18,20-22</sup> The ATRs consist of WM fibers connecting the mediadorsal thalamic nuclei and the frontal cortex, which are frequently affected by HIV pathology.<sup>23</sup> Moreover, these WM tracts are involved in memory encoding and executive functions that may be impaired in HIV patients.<sup>37,38</sup>

ROIs were selected from the JHU WM tractography atlas.<sup>39</sup> From these ROIs, WM masks were generated and projected onto each subject's space using the warping field derived from registering FA values in TBSS process (see above). Special attention was paid to areas close to cerebrospinal fluid (CSF) to avoid contamination of the ROI with freely diffusing CSF and to reduce the risk of partial volume effects. For every subject, mean values and standard deviations of FA, MD, AWF, tortuosity,  $D_{\text{axon}}$ ,  $D_{\text{e,axial}}$ , and  $D_{\text{e,radial}}$  were calculated in each ROI. Voxels corresponding to a T2-hyperintense lesion were excluded from patients' ROIs in both HIV and SPMS patients.

#### *Statistical Analyses*

All the statistical computations were performed using the Statistical Package for Social Sciences (SPSS) version 16.0 (SPSS Inc., Chicago, IL, USA). All data were tested for normal distribution using the Shapiro-Wilk test. Differences in the WMTI measures between the HIV and MS patients were tested with Mann-Whitney U test. Analyses of the relationship between WMTI metrics in the CC and ATRs and neuropsychological

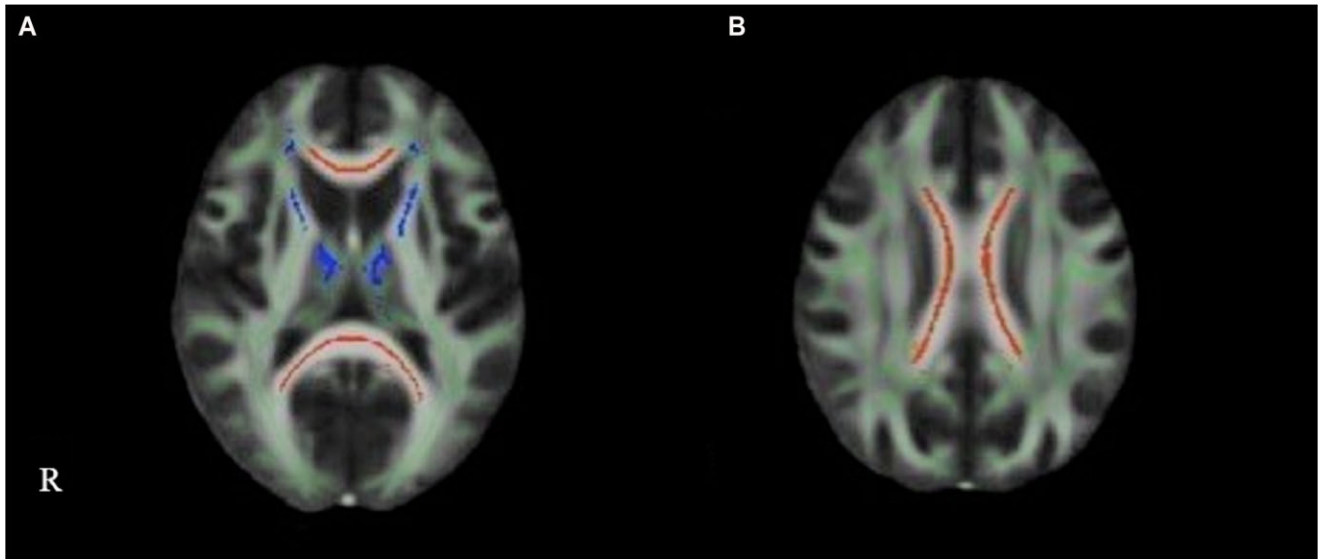


**Fig 2.** Region of interest analysis. Anterior thalamic radiation and corpus callosum masks, derived from the Johns Hopkins University white matter tractography atlas, are shown, respectively, in blue (A) and red (A and B), overlaid on the Oxford Centre for Functional MRI of the brain fractional anisotropy (FA) template. Mean FA skeleton mask obtained from tract-based spatial statistical analysis is shown in green. R = Right.

test scores in HIV patients were performed using Pearson's bivariate correlations taking into account the effect of LV and age. One HIV patient was identified as an outlier and removed from the correlation analyses. Due to the exploratory nature of the study,  $P$  values were not adjusted for multiple comparisons and a value  $\leq .05$  was considered to be statistically significant.

## Results

Five of the HIV patients in the study group had hepatitis C virus (HCV) coinfection, while 6 were affected by HTN and 4 by diabetes. All were on stable antiretroviral therapy, and all but 1 was virally suppressed, with plasma HIV loads under 200 copies/mL. Their median CD4 count was 660 cells/mm<sup>3</sup> (interquartile range [IQR] [399, 922]), with only 2 patients having a current CD4 count under 200. In contrast, the patients had generally low CD4 nadirs in earlier phases of their disease, with the median nadir of 22 (IQR [2-225]). Eleven of the patients had CD4 nadirs of 200 cells/mm<sup>3</sup> or less. Eight patients had a history of opioid addiction and 5 of them were on methadone treatment.

The SPMS patients had a median Expanded Disability Status Scale (EDSS) score of 6.0 (range: 3.0-8.5). None of them was affected by HTN/diabetes/drug abuse.

Clinical data in HIV and SPMS patients are presented in Table 1.

### WM Lesion Volumes

Nine out of 15 HIV patients presented with WM T2 hyperintense lesions. All SPMS patients had WM T2 hyperintense lesions. Mean LV was  $9.29 \pm 9.21$  mL in SPMS patients and was  $8.07 \pm 15.83$  mL in HIV patients. When present, spatial distribution of the lesions was similar between patient groups. Total T2 LVs in both groups are presented in Table 3.

### TBSS Analysis

TBSS analysis revealed widespread differences in terms of WMTI metrics in the WM skeleton of HIV patients compared

Table 3. Total T2 Lesion Volume of the Patient Groups

Patient Group	Total T2 LV in mL
HIV	121.01
SPMS	139.41

HIV = human immunodeficiency virus; SPMS = secondary progressive multiple sclerosis; LV = lesion volume.

to that of SPMS patients. Although SPMS patients showed slightly lower  $D_{e,axonal}$ , AWF, and tortuosity and higher  $D_{e,radial}$  values in several brain regions including the genu, body, and splenium of CC, the superior long fasciculus bilaterally, the left and right ATR, the inferior fronto-occipital fasciculus, and the cingulum, these differences did not survive the threshold-free cluster enhancement correction for multiple comparisons.

### ROI Analysis

#### Corpus Callosum

No statistically significant difference was found between the two groups of patients for any of the WMTI metrics in CC ( $P > .1$ , for all).

#### Right ATR

$D_{e,axial}$  values were significantly lower in HIV patients as compared to SPMS patients ( $P = .003$ ). No difference was found for the other WMTI metrics ( $P > .1$  for all).

#### Left ATR

$D_{e,axial}$  values were significantly lower in HIV patients as compared to SPMS patients ( $P = .003$ ). No significant difference was found in terms of other WMTI metrics ( $P > .1$  for all).

AWF and tortuosity values found positively correlated with the FA values in CC and in the ATRs for both patient groups ( $P < .0001$  for all). Table 4 shows the MRI characteristics of the study groups.

Table 4. MRI Characteristics of the Study Groups

	HIV	SPMS	Effect Size
<b>DTI and DKI metrics in CC</b>			
FA	.64 ± .05	.62 ± .06	.4
MD	.86 ± .18	.88 ± .10	.2
AWF	.45 ± .04	.44 ± .06	.2
Tortuosity	3.07 ± .35	2.89 ± .44	.5
$D_{axon}$	1.16 ± .07	1.14 ± .14	.2
$D_{e,axial}$	2.79 ± .09	2.81 ± .11	.2
$D_{e,radial}$	.93 ± .12	1.01 ± .18	.6
<b>DTI and DKI metrics in the right ATR</b>			
FA	.40 ± .03	.40 ± .04	0
MD	.79 ± .11	.83 ± .14	.3
AWF	.37 ± .03	.38 ± .04	.3
Tortuosity	1.93 ± .16	1.96 ± .15	.2
$D_{axon}$	.72 ± .03	.71 ± .08	.3
$D_{e,axial}$ *	1.99 ± .25	2.11 ± .21	.5
$D_{e,radial}$	1.07 ± .15	1.18 ± .31	.7
<b>DKI metrics in the left ATR</b>			
FA	.39 ± .04	.40 ± .04	.2
MD	.80 ± .16	.82 ± .15	.1
AWF	.38 ± .04	.37 ± .04	.2
Tortuosity	1.88 ± .21	1.95 ± .22	.3
$D_{axon}$	.71 ± .04	.70 ± .08	.2
$D_{e,axial}$ *	1.99 ± .21	2.14 ± .23	.7
$D_{e,radial}$	1.11 ± .25	1.22 ± .34	.4

Asterisks indicate metrics where significant differences found between two groups ( $P < .05$ ). All values are expressed as mean ± standard deviation. HIV = human immunodeficiency virus; SPMS = secondary progressive multiple sclerosis; DKI = diffusion kurtosis imaging; DTI = diffusion tensor imaging; FA = fractional anisotropy; MD = mean diffusivity; AWF = axonal water fraction;  $D_{axon}$  = intra-axonal diffusivity;  $D_{e,axial}$  = axial extra-axonal diffusivity;  $D_{e,radial}$  = radial extra-axonal diffusivity; CC = corpus callosum; ATR = anterior thalamic radiation.

*Correlations between WMTI Parameters and Cognitive Tests in HIV Patients*

$D_{e,radial}$  values in the CC were negatively correlated with TMT-A test scores ( $r = -.69, P = 0.012$ ), whereas they showed a trend toward statistical significance in association with the TMT-B test ( $r = -.51, P = .08$ ). Moreover, tortuosity values showed a trend toward statistical significance in association with TMT-A and

Table 5. Pearson Correlation Coefficients between DKI Metrics and Cognitive Tests in the Corpus Callosum and Anterior Thalamic Radiations

	TMT-A	TMT-B	BVMT DR
<b>CC</b>			
AWF	.38	.22	.08
Tortuosity	.55	.57	.43
$D_{axon}$	.09	.04	.26
$D_{e,axial}$	-.02	-.05	.20
$D_{e,radial}$	-.69*	-.51	-.14
<b>Right ATR</b>			
AWF	.08	-.04	-.34
Tortuosity	.37	.36	.13
$D_{axon}$	-.12	.01	-.17
$D_{e,axial}$	-.15	.27	.50
$D_{e,radial}$	-.13	.17	.56
<b>Left ATR</b>			
AWF	.19	.29	.28
Tortuosity	.32	.50	.34
$D_{axon}$	-.13	.09	.15
$D_{e,axial}$	-.45	.03	.24
$D_{e,radial}$	-.58*	-.20	.26

Asterisks indicate the metrics where a significant correlation found between the DKI metrics and the neuropsychological tests ( $P < .05$ ). DKI = diffusion kurtosis imaging; AWF = axonal water fraction;  $D_{axon}$  = intra-axonal diffusivity;  $D_{e,axial}$  = axial extra-axonal diffusivity;  $D_{e,radial}$  = radial extra-axonal diffusivity; CC = corpus callosum; ATR = anterior thalamic radiation; TMT-A = Trail Making Test-A; TMT-B = Trail Making Test-B; BVMT-DR = brief visuospatial memory test, delayed recall.

TMT-B tests ( $r = .55, P = .06$  and  $r = .57, P = .054$ , respectively). In the left ATR,  $D_{e,radial}$  values were negatively correlated with TMT-A test ( $r = -.58, P = 0.04$ ). (Table 5, Fig 3).

**Discussion**

WM damage assessed by DTI and its clinical and cognitive impact is well documented in patients with HIV.<sup>4,19,40,41</sup> However, in the absence of direct examination of brain tissue, it is difficult to ascertain the specific pathological abnormalities underlying this WM injury. In this study, we sought to further investigate the pathophysiology of WM damage in HIV using DKI-derived

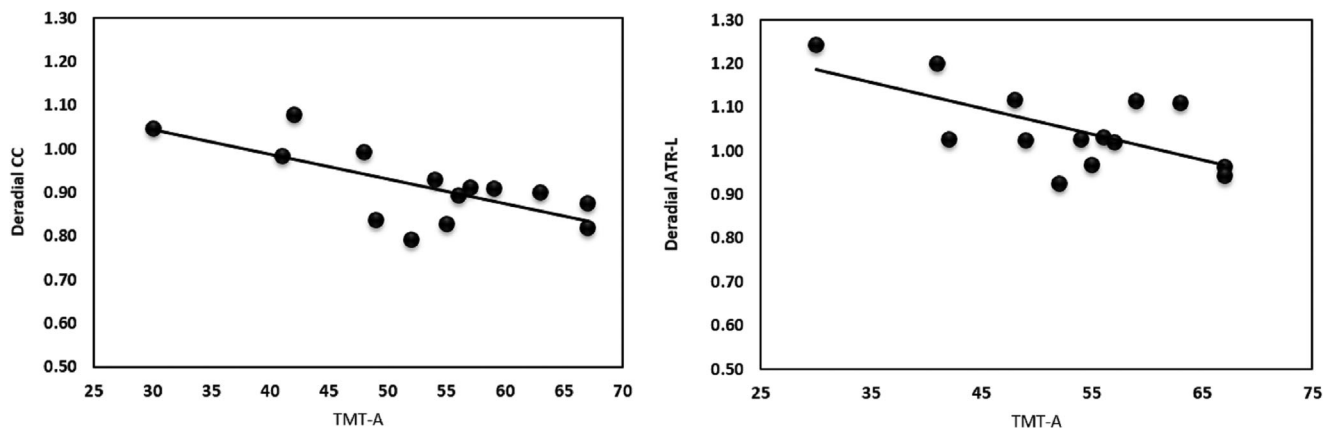


**Fig 3.** Correlations between diffusion kurtosis imaging metrics and the cognitive tests in HIV+ patients. Graphs showing the correlations between white matter tract integrity metrics and standardized cognitive test scores. Specifically, corpus callosum radial extra-axonal diffusivity and Trail Making Test-A scores (a) and left anterior thalamic radiation radial extra-axonal diffusivity and Trail Making Test-A scores (b). ( $P < .05$ ). CC = corpus callosum; ATR-L = left anterior thalamic radiation; TMT-A = trail making test-A;  $D_{e,radial}$  = radial extra-axonal diffusivity.

WMTI metrics that have been shown to be more pathologically specific than DTI-derived metrics in patients with MS.<sup>14,17</sup>

Since HIV pathology shares common features of myelin and axonal damage with that of multiple sclerosis, we selected a group of chronic MS patients as comparators for our pilot study. This is not to imply shared pathogenesis; while both are neuroinflammatory disorders, only rarely are myelin-targeted pathologies encountered in HIV. Furthermore, pathogenesis in HIV has been profoundly impacted by cART and the increasing medical complexity of individuals surviving with persistent viral infection. This is reflected in our patient samples. In contrast to the MS patients, whose only neuroimaging-relevant disorder was their demyelinating CNS disease, the HIV patients had a variety of significant medical comorbidities known to impact WM integrity, such as HCV, HTN, and DM.<sup>42,43</sup> Opioid use might also be independently associated with neurologic, neurocognitive, and neuropathologic complications.<sup>44,45</sup> Furthermore, the HIV patients were representative of the epidemic in New York City, where patients often present with immunologically advanced disease, and are reconstituted through cART therapy. Thus, our HIV patient sample had high-current CD4 T cell counts, but low CD4 T cell nadirs. Thus, given the complexity of our HIV patients and the limited numbers studied in this pilot, we cannot make any inferences regarding the etiology of these changes, and whether they reflect prior HIV-associated damage (as reflected in low CD4 T cell nadir), current HIV-associated disease (with relatively robust CD4 T cells), or HIV-associated medical comorbidity, inclusive of use of potentially neurotoxic drugs in cART.<sup>10</sup> We hope that further study of larger HIV patient populations with this technique will allow us to begin to dissect the complex cellular impacts of HIV and comorbid illnesses that may result in WM alterations on the basis of nonimmunologic conditions such as cerebral small-vessel disease.

Despite the complexity of our HIV patients, it was nevertheless surprising to us when we did not find statistically significant differences in a variety of WMTI metrics between HIV and SPMS patients, suggesting some similar qualitative and quantitative aspects of WM microstructural damage in the two diseases. In both disorders, the degree of chronic axonal loss (AWF) appeared to be similar in all locations assessed. Thus, for the two patient groups with similar length of neurologically relevant disease, the damage to axons appeared commensurate. In contrast, there were regional variations in the relative degree of tortuosity, regionally again attaining the same level of severity in the two groups. Given that HIV is not a primarily demyelinating pathology, this may be an indication that in chronic neuroinflammatory disease, secondary myelin effects may attain comparable severity to disorders with targeted myelin destruction.

From a neuropathological standpoint, patients with progressive MS are characterized by widespread chronic inflammation, astrocytic gliosis, microglial activation, microglial nodules (glial scars), demyelination, and axonal loss.<sup>46</sup> Although the dynamics behind the pathological processes is different, the formation of microglial nodules and multinucleated giant cells in central and deep WM of HIV patients has been associated with the loss of specific neuron subpopulations, synaptic connections, loss of axons, and myelin.<sup>41,46</sup> However, these observations are pertinent to natural history HIV disease; our patients were all cART-treated, and with one exception, had generally low to

undetectable plasma viral loads. This may be thought to constitute a potential weakness of our study, as in this pilot, we did not include a relevant HIV-positive, cART-negative population. Current treatment recommendations are to start cART therapy upon HIV diagnosis; thus, we did not attempt to find a treatment-naïve population for our pilot, as the stably treated group would be more relevant to the larger numbers of people currently living with HIV in our region.

Although preliminary, our study showed an association between measures of WM microstructural abnormalities in the CC and left anterior thalamic tract of HIV patients and measures of executive functioning, visuospatial memory, and information processing speed. Since ATRs are associated with memory encoding, executive functioning,<sup>47</sup> and general cognitive ability,<sup>48</sup> slowed information processing efficiency, executive dysfunction, and deficient episodic memory encoding and retrieval<sup>49</sup> would be expected following WM injury in these regions. Our results confirmed this hypothesis by showing correlations between  $D_{e,radial}$  and tortuosity metrics and cognitive test scores measuring executive functioning and information processing speed in the left ATR. Associations between DKI metrics and cognitive performance that tended to be lateralized to the left hemisphere were previously reported in line with our findings.<sup>5,50</sup>

The main aim of our pilot study was to show the feasibility of using DKI-derived WMTI method on HIV for the first time; thus, we did not select a refined patient group based on more advanced selection criteria, but instead used a convenience sample. We compared the HIV patients with MS patients in regions where WM injury and change of WMTI metrics is very well documented. However, having an age, sex, years of education, and substance abuse behavior matching HC group, an external control would improve our understanding about HIV WM alterations. In the future, to be able to reach broader conclusions regarding the HIV's direct effects on WM microstructure, a study group with no coinfections, medical comorbidity, or substance abuse could be selected. In addition, considering the possible toxic effects of the cART on WMTI, an extra care should be given to control the effect of the treatment on WM microstructure and cognitive performance.

In summary, in this pilot study, we used DKI-derived metrics to characterize WM changes in complex HIV patients; these metrics are thought to provide more pathologically specific measures of WMTI than classical DTI metrics. The overall WMTI pattern of HIV patients showed similarities in axonal loss and myelin damage with chronic MS, despite their different etiologies. Similar to prior studies of HIV with DTI, DKI-derived metrics showed preliminary correlation with HIV-associated cognitive abnormality. Detection of WM abnormality using new measures of microstructural alterations such as AWF and tortuosity may help to understand/characterize the WM pathology and cognitive disorders in HIV more comprehensively, thus providing greater insight into HIV neuropathogenesis.

## References

1. Wright PW, Heaps JM, Shimony JS, et al. The effects of HIV and combination antiretroviral therapy on white matter integrity. *AIDS* 2012;26:1501-8.
2. Filippi CG, Ulug AM, Ryan E, et al. Diffusion tensor imaging of patients with HIV and normal-appearing white matter on MR images of the brain. *AJNR Am J Neuroradiol* 2001;22:277-83.

3. Langford TD, Letendre SL, Larrea GJ, et al. Changing patterns in the neuropathogenesis of HIV during the HAART era. *Brain Pathol* 2003;13:195-210.
4. Wohlschlaeger J, Wenger E, Mehraein P, et al. White matter changes in HIV-1 infected brains: a combined gross anatomical and ultrastructural morphometric investigation of the corpus callosum. *Clin Neurol Neurosurg* 2009;111:422-9.
5. Zhu T, Zhong J, Hu R, et al. Patterns of white matter injury in HIV infection after partial immune reconstitution: a DTI tract-based spatial statistics study. *J Neurovirol* 2013;19:10-23.
6. Antinori A, Arendt G, Becker JT, et al. Updated research nosology for HIV-associated neurocognitive disorders. *Neurology* 2007;69:1789-99.
7. Woods SP, Moore DJ, Weber E, et al. Cognitive neuropsychology of HIV-associated neurocognitive disorders. *Neuropsychol Rev* 2009;19:152-68.
8. Heaton RK, Franklin DR, Ellis RJ, et al. HIV-associated neurocognitive disorders before and during the era of combination antiretroviral therapy: differences in rates, nature, and predictors. *J Neurovirol* 2011;17:3-16.
9. Ellero J, Lubomski M, Brew B. Interventions for neurocognitive dysfunction. *Curr HIV/AIDS Rep* 2017;14:8-16.
10. Robertson K, Liner J, Meeker RB. Antiretroviral neurotoxicity. *J Neurovirol* 2012;18:388-99.
11. Pomara N, Crandall DT, Choi SJ, et al. White matter abnormalities in HIV-1 infection: a diffusion tensor imaging study. *Psychiatry Res* 2001;106:15-24.
12. Fieremans E, Jensen JH, Helpers JA. White matter characterization with diffusional kurtosis imaging. *Neuroimage* 2011;58:177-88.
13. Jensen JH, Helpers JA, Ramani A, et al. Diffusional kurtosis imaging: the quantification of non-gaussian water diffusion by means of magnetic resonance imaging. *Magn Reson Med* 2005;53:1432-40.
14. Struyfs H, Van Hecke W, Veraart J, et al. Diffusion kurtosis imaging: a possible MRI biomarker for AD diagnosis? *J Alzheimers Dis* 2015;48:937-48.
15. Hui ES, Fieremans E, Jensen JH, et al. Stroke assessment with diffusional kurtosis imaging. *Stroke* 2012;43:2968-73.
16. Ito K, Sasaki M, Ohtsuka C, et al. Differentiation among parkinsonisms using quantitative diffusion kurtosis imaging. *Neuroreport* 2015;26:267-72.
17. de Kouchkovsky I, Fieremans E, Fleysher L, et al. Quantification of normal-appearing white matter tract integrity in multiple sclerosis: a diffusion kurtosis imaging study. *J Neurol* 2016;263:1146-55.
18. Bester M, Jensen JH, Babb JS, et al. Non-Gaussian diffusion MRI of gray matter is associated with cognitive impairment in multiple sclerosis. *Multi Scler J* 2015;21:935-44.
19. Masters MC, Ances BM. Role of neuroimaging in HIV-associated neurocognitive disorders. *Semin Neurol* 2014;34:89-102.
20. Leite SC, Correa DG, Doring TM, et al. Diffusion tensor MRI evaluation of the corona radiata, cingulate gyri, and corpus callosum in HIV patients. *J Magn Reson Imaging* 2013;38:1488-93.
21. Wright PW, Vaida FF, Fernandez RJ, et al. Cerebral white matter integrity during primary HIV infection. *AIDS* 2015;29:433-42.
22. Ozturk A, Smith SA, Gordon-Lipkin EM, et al. MRI of the corpus callosum in multiple sclerosis: association with disability. *Multi Scler J* 2010;16:166-77.
23. Correa DG, Zimmermann N, Doring TM, et al. Diffusion tensor MR imaging of white matter integrity in HIV-positive patients with planning deficit. *Neuroradiology* 2015;57:475-82.
24. Lublin FD. New multiple sclerosis phenotypic classification. *Eur Neurol* 2014;72(Suppl 1):1-5.
25. Woods SP, Rippeth JD, Frol AB, et al. Interrater reliability of clinical ratings and neurocognitive diagnoses in HIV. *J Clin Exp Neuropsychol* 2004;26:759-78.
26. Fellows RP, Byrd DA, Morgello S. Effects of information processing speed on learning, memory, and executive functioning in people living with HIV/AIDS. *J Clin Exp Neuropsychol* 2014;36:806-17.
27. Inglese M, Madelin G, Oesingmann N, et al. Brain tissue sodium concentration in multiple sclerosis: a sodium imaging study at 3 tesla. *Brain* 2010;133:847-57.
28. Andersson JLR, Skare S, Ashburner J. How to correct susceptibility distortions in spin-echo echo-planar images: application to diffusion tensor imaging. *NeuroImage* 2003;20:870-88.
29. Smith SM, Jenkinson M, Woolrich MW, et al. Advances in functional and structural MR image analysis and implementation as FSL. *Neuroimage* 2004;23(Suppl 1):S208-19.
30. Graham MS, Drobnyak I, Zhang H. Realistic simulation of artefacts in diffusion MRI for validating post-processing correction techniques. *NeuroImage* 2016;125:1079-94.
31. Smith SM. Fast robust automated brain extraction. *Hum Brain Mapp* 2002;17:143-55.
32. Tabesh A, Jensen JH, Ardekani BA, et al. Estimation of tensors and tensor-derived measures in diffusional kurtosis imaging. *Magn Reson Med* 2011;65:823-36.
33. Smith SM, Jenkinson M, Johansen-Berg H, et al. Tract-based spatial statistics: voxelwise analysis of multi-subject diffusion data. *Neuroimage* 2006;31:1487-505.
34. Smith SM, Jenkinson M, Woolrich MW, et al. Advances in functional and structural MR image analysis and implementation as FSL. *Neuroimage* 2004;23(Suppl 1):S208-19.
35. Andersson JLR, Jenkinson M, Smith S. *Non-linear registration aka spatial normalisation*. Oxford, UK: FMRIB Centre, 2007. Available at: [www.fmrib.ox.ac.uk/datasets/techrep/tr07ja2/tr07ja2.pdf](http://www.fmrib.ox.ac.uk/datasets/techrep/tr07ja2/tr07ja2.pdf)
36. Smith SM, Nichols TE. Threshold-free cluster enhancement: addressing problems of smoothing, threshold dependence and localisation in cluster inference. *NeuroImage* 2009;44:83-98.
37. Zhou Y, Fan L, Qiu C, et al. Prefrontal cortex and the dysconnectivity hypothesis of schizophrenia. *Neurosci Bull* 2015;31:207-19.
38. Mamah D, Conturo TE, Harms MP, et al. Anterior thalamic radiation integrity in schizophrenia: a diffusion-tensor imaging study. *Psychiatry Res* 2010;183:144-50.
39. Hua K, Zhang J, Wakana S, et al. Tract probability maps in stereotaxic spaces: analyses of white matter anatomy and tract-specific quantification. *Neuroimage* 2008;39:336-47.
40. Seider TR, Gongvatana A, Woods AJ, et al. Age exacerbates HIV-associated white matter abnormalities. *J Neurovirol* 2016;22:201-12.
41. Su T, Caan MWA, Wit FWNM, et al. White matter structure alterations in HIV-1-infected men with sustained suppression of viraemia on treatment. *AIDS* 2016;30:311-22.
42. Smith AB, Smirniotopoulos JG, Rushing EJ. From the archives of the AFIP: central nervous system infections associated with human immunodeficiency virus infection: radiologic-pathologic correlation. *Radiographics* 2008;28:2033-58.
43. Solinas A, Piras MR, Deplano A. Cognitive dysfunction and hepatitis C virus infection. *World J Hepatol* 2015;7:922-5.
44. Byrd DA, Fellows RP, Morgello S, et al. Neurocognitive impact of substance use in HIV infection. *J Acquir Immune Defic Syndr* 2011;58:154-62.
45. Byrd D, Murray J, Safdieh G, et al. Impact of opiate addiction on neuroinflammation in HIV. *J Neurovirol* 2012;18:364-73.
46. Lassmann H, van Horssen J, Mahad D. Progressive multiple sclerosis: pathology and pathogenesis. *Nat Rev Neurol* 2012;8:647-56.
47. Mamah D, Conturo TE, Harms MP, et al. Anterior thalamic radiation integrity in schizophrenia: a diffusion-tensor imaging study. *Psychiatry Res* 2010;183:144-50.
48. Booth T, Bastin ME, Penke L, et al. Brain white matter tract integrity and cognitive abilities in community-dwelling older people: the Lothian Birth Cohort, 1936. *Neuropsychology* 2013;27:595-607.
49. Reger M, Welsh R, Razani J, et al. A meta-analysis of the neuropsychological sequelae of HIV infection. *J Int Neuropsychol Soc* 2002;8:410-24.
50. Melrose RJ, Tinaz S, Castelo JM, et al. Compromised fronto-striatal functioning in HIV: an fMRI investigation of semantic event sequencing. *Behav Brain Res* 2008;188:337-47.